The Ideal MIMO Channel: Maximizing Capacity in Sparse Multipath with Reconfigurable Arrays

Akbar M. Sayeed and Vasanthan Raghavan
Department of Electrical and Computer Engineering
University of Wisconsin-Madison
akbar@engr.wisc.edu, vraghavan@cae.wisc.edu

***Abstract*— While the intense research on multi-antenna (MIMO) wireless communication channels was pioneered by results based on an i.i.d. channel model representing a rich multipath environment, there is growing experimental evidence that physical wireless channels exhibit a sparse multipath structure, even at relatively low antenna dimensions. In this paper, we propose a model for sparse multipath channels and study coherent MIMO capacity as a function of SNR for a fixed number of antennas. In a recent work, we had shown that the spatial distribution of the sparse multipath has a significant impact on capacity and had also characterized the optimal distribution (the Ideal MIMO Channel) that maximizes capacity at any operating SNR. In this paper, we refine these results and develop a framework for maximizing MIMO capacity at any SNR by *systematically* adapting the array configurations (antenna spacings) at the transmitter and receiver to the level of sparsity. Surprisingly, three canonical array configurations are sufficient for near-optimum performance over the entire SNR range. In a scattering environment with randomly distributed paths, the capacity gain due to optimal configuration is directly proportional to the number of antennas at low SNR's. Numerical results based on a realistic physical model are presented to illustrate capacity gains with reconfigurable antenna arrays.**

I. Introduction

While the intense research on multi-antenna (MIMO) wireless communication systems was pioneered by initial results in rich multipath environments [1], [2], there is growing evidence that physical wireless channels exhibit a *sparse* structure even at relatively small antenna dimensions [7], [3]. In this paper we show that the sparsity of multipath can be exploited for dramatically increasing MIMO capacity at low SNR's by matching the array configurations (antenna spacings) to the level of sparsity. We focus on uniform linear arrays (ULAs) of antennas and provide a systematic characterization of the impact of antenna spacing on coherent capacity. Our results confirm and extend recent studies that indicate that in certain correlated environments reducing the antenna spacings can actually increase capacity and that this effect is most pronounced in the low-SNR regime [3], [8], [9]. Furthermore, technological advances in reconfigurable antenna arrays are enabling new wireless communication devices in which the array configuration can be adapted to changes in the communication environment. Thus, understanding the impact of reconfigurable arrays on MIMO capacity, and developing strategies for sensing and adapting to the environment, is of significant interest both theoretically and practically.

Our approach is based on the virtual channel representation [5] that provides an accurate and analytically tractable model for physical wireless channels. Let $\mathbf{H}$ denote an $N \times N$ virtual channel matrix representing N antennas at the transmitter and the receiver. The dominant non-vanishing entries of the virtual channel matrix reveal the statistically independent degrees of freedom (DoF), D, in the channel which also represent the number of resolvable paths in the scattering environment. For sparse channels, $D < N^2$, as illustrated in Fig. 1(a). The contributions of this paper build on our recent results in [3] in which we revisited coherent capacity *scaling* in MIMO channels with N and argued that the DoF (and channel power) can at best scale at a *sub-quadratic* rate, $D(N) = o(N^2)$, and consequently the capacity of physical channels can at best scale at a *sub-linear* rate which cannot exceed $\mathcal{O}\left(\sqrt{D(N)}\right) = o(N)$. We also introduced the notion of an ideal MIMO channel that achieves $\mathcal{O}\left(\sqrt{D(N)}\right)$ scaling.

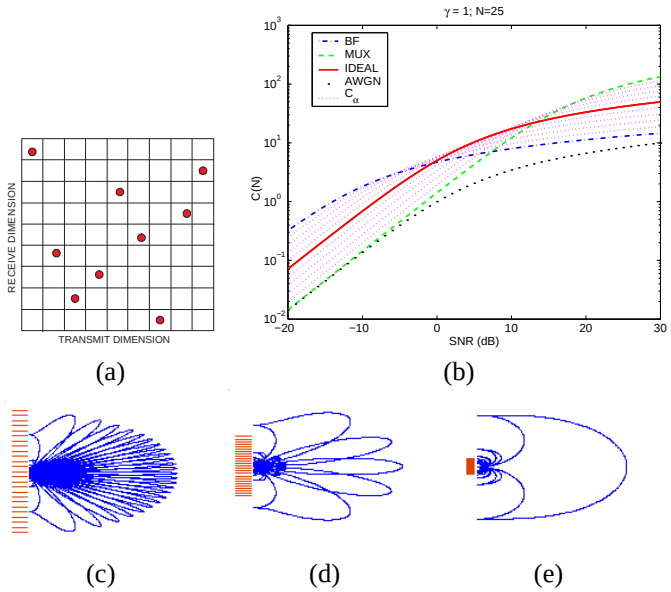

Fig. 1. (a) A sparse 9 x 9 virtual channel matrix. (b) Capacity versus SNR for different channel configurations for D=N=25. (c)-(e): Virtual beam directions for $N = 25$ and different spacings; (c) large spacing; (d) medium spacing; (e) small spacing.

The results in [3] also revealed a fundamental new tradeoff in sparse channels between the multiplexing gain (MG; the

number of parallel channels) and the received SNR per parallel channel that governs channel capacity *as a function of SNR* for a *fixed* N. We introduced a family of channel described by two parameters (p, q), $D = pq$, that represents different configurations of the $D < N^2$ DoF. We showed that for all feasible (p, q) the MIMO capacity of the corresponding channel configuration is accurately approximated by

$$C(N, \rho, D, p) \approx p \log(1 + \rho D/p^2) \tag{1}$$

where ρ denotes the transmit SNR, p represents the MG, $q = D/p$ represents the DoF per parallel channel, and $\rho D/p^2 = \rho q/p = \rho_{rx}$ denotes the received SNR per parallel channel. Thus, increasing p comes at the cost of ρ_{rx} and vice versa. This is illustrated in Fig. 1(b) where there dotted curves represent different values of p. The most important observation is that for any ρ there is an optimum channel configuration (value of p) that optimizes the MG-SNR tradeoff and yields the highest capacity. We term this optimal configuration as the *Ideal MIMO Channel* at the particular SNR.

Summary of Results. In this paper, we refine the concept of the Ideal MIMO Channel and develop a framework for maximizing capacity in sparse environments by *systematically* adapting the antenna spacings at the transmitter (Tx) and receiver (Rx).[1] Unlike existing characterizations of the capacity-maximizing input, that are explicit only in low- or high-SNR regimes, our results characterize the capacity-maximizing array configurations and corresponding optimal signaling schemes for all SNR's. Surprisingly, only three canonical array configurations are sufficient for near-optimum performance over the entire SNR range. The multiplexing (MUX) configuration ($p = p_{max} = N$) in Fig. 1(b) is optimal at high SNR, $\rho > \rho_{high}$, and is realized by sufficiently large spacings at both ends, illustrated in Fig. 1(c). The beamforming (BF) configuration ($p = p_{min} = 1$) is optimal at low SNR, $\rho < \rho_{low}$, and is realized by closely spaced antennas at the Tx (Fig. 1(e)) and large spacing at the Rx (Fig. 1(c)). The IDEAL configuration ($p = p_{id} = \sqrt{N}$) that yields the *fastest capacity scaling* [3] is a robust choice for $\rho \in (\rho_{low}, \rho_{high})$ and is realized by medium spacings at the Tx and the Rx (Fig. 1(d)). As evident, the capacity gains achievable by adapting antenna spacings to channel sparsity are very substantial, especially in the low-SNR regime. We quantify these gains, illustrate the results with a realistic numerical simulation, and provide a *physical source-channel matching* interpretation of the proposed methodology.

II. Virtual Modeling of Multipath Channels

We consider a single-user MIMO system with ULA's of N_t transmit and N_r receive antennas. The transmitted signal $\mathbf{s}$ and the received signal $\mathbf{x}$ are related by $\mathbf{x} = \mathbf{H}\mathbf{s} + \mathbf{n}$ where $\mathbf{H}$ is the MIMO channel matrix and $\mathbf{n}$ is the AWGN at the receiver.

[1]We noted this possibility in [3] and suggested a form of adaptive-resolution spatial signaling for achieving it. However, the approach in [3] makes implicit assumptions on power amplification at the transmitter, which may not be feasible. The approach presented here circumvents those assumptions.

A physical multipath channel can be accurately modeled as

$$\mathbf{H} = \sum_{\ell=1}^{L} \beta_\ell \ \mathbf{a}_r(\theta_{r,\ell}) \mathbf{a}_t^H(\theta_{t,\ell}) \tag{2}$$

where the transmitter and receiver arrays are coupled through L propagation paths with complex path gains $\{\beta_\ell\}$, Angles of Departure (AoD) $\{\theta_{t,\ell}\}$ and Angles of Arrival (AoA) $\{\theta_{r,\ell}\}$. In (2), $\mathbf{a}_r(\theta_r)$ and $\mathbf{a}_t(\theta_t)$ denote the receiver response and transmitter steering vectors for receiving/transmitting in the normalized direction θ_r/θ_t, where θ is related to the physical angle (in the plane of the arrays) $\phi \in [-\pi/2, \pi/2]$ as $\theta = d \sin(\phi)/\lambda$, d is the antenna spacing and λ is the wavelength of propagation. Both $\mathbf{a}_r(\theta_r)$ and $\mathbf{a}_t(\theta_t)$ are periodic in θ with period 1 [5].

The *virtual MIMO channel representation* [5] characterizes a physical channel via coupling between spatial beams in fixed virtual transmit and receive directions

$$\mathbf{H} = \sum_{m=1}^{N_r} \sum_{n=1}^{N_t} H_v(m,n) \mathbf{a}_r(\tilde{\theta}_{r,m}) \mathbf{a}_t^H(\tilde{\theta}_{t,n}) = \mathbf{A}_r \mathbf{H}_v \mathbf{A}_t^H \tag{3}$$

where $\left\{\tilde{\theta}_{r,m} = \frac{m}{N_r}\right\}$ and $\left\{\tilde{\theta}_{t,n} = \frac{n}{N_t}\right\}$ are fixed virtual receive and transmit angles that uniformly sample the unit θ period and result in unitary (DFT) matrices $\mathbf{A}_t$ and $\mathbf{A}_r$. Thus, $\mathbf{H}$ and $\mathbf{H}_v$ are unitarily equivalent: $\mathbf{H}_v = \mathbf{A}_r^H \mathbf{H} \mathbf{A}_t$. The virtual representation is linear and is characterized by the matrix $\mathbf{H}_v$.

The virtual representation induces a partitioning of propagation paths [5]: each $\mathbf{H}_v(m,n)$ is associated with a disjoint set of physical paths and is approximately equal to the sum of the gains of the corresponding paths. It follows that the virtual channel coefficients are approximately independent and we assume that the virtual channel coefficients are statistically independent zero-mean Gaussian random variables.

A. Transmit, Receive and Joint Channel Statistics

Channel statistics play a key role in our characterization of optimal array configurations. In Rayleigh fading, the statistics of $\mathbf{H}$ are characterized by the virtual channel power matrix $\mathbf{\Psi}$: $\mathbf{\Psi}(m,n) = E[|\mathbf{H}_v(m,n)|^2]$. The matrices $\mathbf{A}_r$ and $\mathbf{A}_t$ constitute the matrices of eigenvectors for the transmit and receive covariance matrices, respectively: $E[\mathbf{H}^H\mathbf{H}] = \mathbf{A}_t \mathbf{\Lambda}_t \mathbf{A}_t^H$ and $E[\mathbf{H}\mathbf{H}^H] = \mathbf{A}_r \mathbf{\Lambda}_r \mathbf{A}_r^H$, where $\mathbf{\Lambda}_t = E[\mathbf{H}_v^H \mathbf{H}_v]$ and $\mathbf{\Lambda}_r = E[\mathbf{H}_v \mathbf{H}_v^H]$ are the diagonal matrices of transmit and receive eigenvalues (correlation matrices in the virtual domain). We can interpret $\mathbf{\Psi}$ as the joint distribution of channel power as a function of transmit and receive virtual angles. $\mathbf{\Lambda}_t$ and $\mathbf{\Lambda}_r$ serve at the corresponding marginal distributions: $\mathbf{\Lambda}_r(m) = \sum_n \mathbf{\Psi}(m,n)$ and $\mathbf{\Lambda}_t(n) = \sum_m \mathbf{\Psi}(m,n)$.

B. Sparse Virtual Channels

We consider $N = N_r = N_t$ for the rest of the paper. Measurements studies have shown that the dominant virtual coefficients tend to be sparse (see, e.g., [7]) even for relatively small $N \sim 8$. We abstract the notion of sparsity in the following definition.

Definition 1 (Sparse Virtual Channels): An $N \times N$ $\mathbf{H}_v$ is sparse if it contains $D < N^2$ non-vanishing coefficients. We assume that each non-vanishing coefficients $\mathcal{CN}(0,1)$ reflecting the power contributed by the *unresolvable* paths associated with it. D reflects the statistically independent DoF in the channel and the channel power $\rho_c(N) = E\left[\mathrm{tr}(\mathbf{H}_v\mathbf{H}_v^H)\right] = \sum_{\ell=1}^{L} E|\beta_\ell|^2 = D$. □

Sparse virtual channel matrices provide a model for spatial correlation in $\mathbf{H}$: in general, the sparser the $\mathbf{H}_v$ in the virtual domain, the higher the correlation in the antenna domain $\mathbf{H}$. It is convenient to model a sparse $\mathbf{H}_v$ as

$$\mathbf{H}_v = \mathbf{M} \odot \mathbf{H}_{iid} \tag{4}$$

where $\odot$ denotes element-wise product, $\mathbf{H}_{iid}$ is an i.i.d. matrix with $\mathcal{CN}(0,1)$ entries, and $\mathbf{M}$ is a mask matrix with D unit entries and zeros elsewhere. Under these assumptions, $\mathbf{\Psi} = \mathbf{M}$ and the entries of $\mathbf{\Lambda}_r$ and $\mathbf{\Lambda}_t$ represent the number of non-zero elements in the rows and columns of $\mathbf{M}$, respectively.

C. Capacity-Achieving Input

The ergodic capacity of a MIMO channel, assuming knowledge of $\mathbf{H}$ at the receiver, is given by [1], [2]

$$C(N,\rho) = \max_{\mathrm{Tr}(\mathbf{Q})\le\rho} E_{\mathbf{H}_v}\left[\log\det\left(\mathbf{I} + \mathbf{H}_v\mathbf{Q}\mathbf{H}_v^H\right)\right] \tag{5}$$

where ρ is the transmit SNR, and $\mathbf{Q} = E[\mathbf{s}\mathbf{s}^H]$ is the transmit covariance matrix. It is shown in [6] that the capacity-maximizing $\mathbf{Q}_{opt}$ is diagonal. Furthermore, for general (non-regular [4]) correlated channels, $\mathbf{Q}_{opt}$ is full-rank at high SNR's, whereas it is rank-1 (beamforming) at low SNR's. As ρ is increased from low to high SNR's, the rank of $\mathbf{Q}_{opt}$ increases from 1 to N.

III. The Ideal MIMO Channel

The capacity of a sparse virtual channel matrix $\mathbf{H}_v$ depends on three fundamental quantities: 1) the transmit SNR ρ, 2) the number of DoF, $D < N^2$, and 3) the distribution of the D DoF in the available N^2 dimensions. Our asymptotic results on capacity scaling in [3] indicated that for any ρ there is an optimal configuration of the DoF, characterized by an optimal mask matrix $\mathbf{M}_{opt}$, that yields the highest capacity at that ρ. We term the corresponding MIMO channel the Ideal MIMO Channel and the resulting capacity the ideal MIMO capacity at that ρ.

Definition 2 (Ideal MIMO Channel): Consider a fixed N and $D < N^2$ and let $\mathcal{M}(D)$ denote the set of all $N \times N$ mask matrices with D non-zero (unit) entries. For any ρ, the ideal MIMO capacity is defined as

$$C_{id}(N,D,\rho) = \max_{\mathbf{M}\in\mathcal{M}(D)} C(N,\rho,\mathbf{M}) \tag{6}$$

and an $\mathbf{M}_{opt}$ that achieves $C_{id}(N,D,\rho)$ defines the Ideal MIMO Channel at that ρ. □

$\mathbf{M}_{opt}$ is not unique in general. In [3] we presented an explicit family of mask matrices to characterize a particular $\mathbf{M}_{opt}$ for any given ρ. The family of mask matrices is defined by two parameters (p,q) such that $D = pq$. For $D = N^\gamma$, $\gamma \in [0,2]$, the matrices can be further parameterized via $p = N^\alpha$, $\alpha \in [\alpha_{min}, \alpha_{max}]$ where $\alpha_{min} = \max(\gamma - 1, 0)$ and $\alpha_{max} = \min(\gamma, 1)$, and $q = D/p$. The mask matrices are illustrated in Fig. 2 for $\gamma \in [1,2]$. The following proposition summarizes the properties of the mask matrices relevant to this paper.

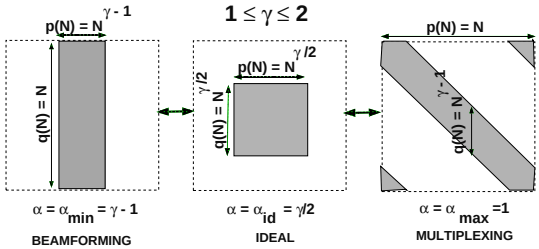

Fig. 2. A family of mask matrices. $\gamma \in [1,2]$.

Proposition 1: For a given $D = N^\gamma$, $\gamma \in [0,2]$, and any $p = N^\alpha$, $\alpha \in [\alpha_{min}, \alpha_{max}]$, the mask matrix $\mathbf{M}(D,p)$ is an $N \times N$ matrix but its non-zero entries are contained in a non-zero sub-matrix of size $r \times p$, $r = \max(q,p)$, consisting of p non-zero columns, and q non-zero (unit) entries in each column. The corresponding $r \times p$ virtual sub-matrices $\tilde{\mathbf{H}}_v$ defined by (4) satisfy $\rho_c = D$ and their transmit and receive correlation matrices are given by

$$\tilde{\mathbf{\Lambda}}_t = E[\tilde{\mathbf{H}}_v^H\tilde{\mathbf{H}}_v] = \frac{D}{p}\mathbf{I}_p = q\mathbf{I}_p \tag{7}$$

$$\tilde{\mathbf{\Lambda}}_r = E[\tilde{\mathbf{H}}_v\tilde{\mathbf{H}}_v^H] = \frac{D}{r}\mathbf{I}_r = \begin{cases} p\mathbf{I}_q & , \quad q \ge p \\ q\mathbf{I}_p & , \quad q < p \end{cases} \quad \square \tag{8}$$

Corollary 1: Since each $\tilde{\mathbf{H}}_v$ defines a regular channel [4], the capacity maximizing input allocates uniform power over the non-vanishing transmit dimensions, $\tilde{\mathbf{Q}}_{opt} = \frac{\rho}{p}\mathbf{I}_p$, and no power in the remaining dimensions.

We showed in [3] that the channel capacity for any $\mathbf{M}(D,p)$ is characterized by the formula (1) which was derived for large N but yields accurate estimates even for relatively small N. The following theorem, which can be inferred form the result in [3], characterizes the mask matrix associated with the Ideal MIMO Channel at any ρ.

Theorem 1: For sufficiently large N, the capacity of the MIMO channel defined by the mask $\mathbf{M}(D,p)$ is accurately approximated as a function of ρ by

$$C(N,\rho,\mathbf{M}(D,p)) \approx p\log\left(1 + \rho\frac{D}{p^2}\right) \tag{9}$$

For a given ρ, the Ideal MIMO Channel is characterized by $\mathbf{M}(D,p_{opt}) \leftrightarrow p_{opt}$ where

$$p_{opt} \approx \begin{cases} p_{min} & , \quad \rho < \rho_{low} \\ \frac{\sqrt{\rho D}}{2} & , \quad \rho \in [\rho_{low}, \rho_{high}] \\ p_{max} & , \quad \rho > \rho_{high} \end{cases} \tag{10}$$

and $C_{id}(N,D,\rho) = C(N,\rho,\mathbf{M}(D,p_{opt}))$. In (10), $p_{min} = N^{\alpha_{min}}$, $p_{max} = N^{\alpha_{max}}$, $\rho_{low} \approx 4p_{min}^2/D = 4N^{2\alpha_{min}}/D$ and $\rho_{high} \approx 4p_{max}^2/D = 4N^{2\alpha_{max}}/D$. □

Remark 1: Different values of p reveal a multiplexing gain (MG) versus received SNR tradeoff. In (9), $\rho D/p^2 =$

$\frac{E[\|\mathbf{Hs}\|^2]}{p} = \rho_{rx}$ is the received SNR per parallel channel [3]. Thus increasing the MG comes at the cost of a reduction in ρ_{rx} and vice versa. For $\rho < \rho_{low}$, the optimal configuration (BF in Fig. 1; $p = p_{min}$) maximizes ρ_{rx}, whereas for $\rho > \rho_{high}$, the optimal configuration (MUX in Fig. 1; $p = p_{max}$) maximizes the MG. The optimal choice p_{opt} for $\rho \in (\rho_{min}, \rho_{max})$ reflects a judicious balance between MG and ρ_{rx}.

The ratio $\rho_{high}/\rho_{low} = (p_{max}/p_{min})^2$ attains its largest value, N^2, for $\gamma = 1$ ($D = N$), whereas it achieves its minimum value of unity for $\gamma = 0$ ($D = 1$) or $\gamma = 2$ ($D = N^2$). Thus, the MG-ρ_{rx} tradeoff does not exist for the extreme cases of highly correlated ($\gamma = 0$) and i.i.d. ($\gamma = 2$) channels. On the other hand, the impact of the MG-ρ_{rx} tradeoff on capacity is highest for $\gamma = 1$ ($D = N$).

IV. Maximizing Capacity with Reconfigurable Antenna Arrays

In this section we present a systematic approach for maximizing MIMO capacity in sparse multipath environments by varying the antenna spacings at the transmitter (d_t) and receiver (d_r). We focus on $D = N^\gamma$, $\gamma \in [1, 2)$, since for $\gamma \in (0, 1)$, it is advantageous to use fewer antennas to effectively increase γ to 1 (see Rem. 1). We first define the notion of randomly sparse physical channels.

Definition 3 (Randomly Sparse Physical Channels): For a given array dimension N, a class $\mathcal{H}(D)$ of channels is said to be randomly sparse with D degrees of freedom if it contains $L = D < N^2$ resolvable paths that are randomly distributed over the maximum angular spreads for sufficiently large antenna spacings $d_{t,max}$ and $d_{r,max}$; that is, $(\theta_{r,\ell}, \theta_{t,\ell}) \in [-1/2, 1/2] \times [-1/2, 1/2]$ in (2). We assume that all paths have $\mathcal{CN}(0, 1)$ path gains $\{\beta_\ell\}$ (Rayleigh fading). □

The maximum antenna spacings serve as an anchor point for relating to the ideal MIMO development in Sec. III and correspond to the choice $p = p_{max} = N$ (MUX configuration); that is, $(d_{t,max}, d_{r,max}) \leftrightarrow p_{max}$. For such a randomly sparse scattering environment, the next result describes the required antenna spacings to create a MIMO channel whose transmit and receive statistics match those induced by $\mathbf{M}(D, p)$ for any desired p as in Prop. 1 and Thm. 1.

Theorem 2: Consider the class of randomly sparse physical channels with $D = N^\gamma$, $\gamma \in [1, 2)$, DoF. For any p, $p_{min} \le p \le p_{max}$, define the antennas spacings

$$d_t = \frac{p d_{t,max}}{N} \quad , \quad d_r = \frac{r d_{r,max}}{N} \tag{11}$$

where $r = \max(q, p)$ and $q = D/p$. Then, for each p, the non-vanishing entries of the resulting $\mathbf{H}_v$ are contained within an $r \times p$ sub-matrix $\tilde{\mathbf{H}}_v$ with power matrix $\tilde{\mathbf{\Psi}} = \frac{D}{pr}\mathbf{1}_{r\times p}$. Furthermore, the transmit and receive correlation matrices, $\tilde{\mathbf{\Lambda}}_t$ and $\tilde{\mathbf{\Lambda}}_r$, respectively, of $\tilde{\mathbf{H}}_v$ match those generated by the mask matrix $\mathbf{M}(D, p)$ as in Prop. 1.

Proof: First, using (2) it is easy to show that, for a given scattering environment, the channel power does not change with antenna spacing. By assumption we have $\rho_c = \mathrm{tr}(E[\mathbf{H}_v\mathbf{H}_v^H]) = D$. Also by assumption, the D randomly distributed paths cover maximum angular spreads (AS's) at the maximum spacings. Since $\theta = d\sin(\phi)/\lambda$, where ϕ is the physical angle associated with a path (which remains unchanged), the d_r and d_t in (11) result in smaller AS's: $[-p/2N, p/2N]$ at the transmitter and $[-r/2N, r/2N]$ at the receiver. Since the spacing between virtual angles is $\Delta\theta = 1/N$, it follows that only $p = p/N/\Delta\theta$ virtual angles lie within the reduced AS at the transmitter and only r virtual angles lie within the reduced angular spread at the receiver. Thus, the non-zero entries in $\mathbf{H}_v$ are contained in a sub-matrix $\tilde{\mathbf{H}}_v$ of size $r \times p$. The channel power $\rho_c = D$ is uniformly distributed over its entries so that $E[|\tilde{\mathbf{H}}_v(m, n)|^2] = \frac{D}{rp}$, $\tilde{\mathbf{\Lambda}}_r = E[\tilde{\mathbf{H}}_v\tilde{\mathbf{H}}_v^H] = (D/r)\mathbf{I}_r$ and $\mathbf{\Lambda}_t = E[\tilde{\mathbf{H}}_v^H\tilde{\mathbf{H}}_v] = q\mathbf{I}_p$, where the expectation is over the statistics of the D non-vanishing coefficients as well as their random locations. The proposition thus follows by comparison with Prop. 1 for $\gamma \in [1, 2)$ ■

Corollary 2: The power matrix of the reconfigured channel corresponding to the spacings in (11) satisfies: $\mathbf{\Psi} = \mathbf{M}(D, p)$ for $p \le \sqrt{D}$ ($q \ge p$), but $\mathbf{\Psi} \ne \mathbf{M}(D, p)$ for $p > \sqrt{D}$ ($q < p$).

Remark 2: **Ideal MIMO Capacity.** Thm. 2 and Cor. 2 imply that in randomly sparse physical channels, the virtual channel matrix generated by reconfiguring antenna spacings has identical statistics (marginal and joint) to those generated by the mask matrix $\mathbf{M}(D, p)$ for $p \le q$, but only the marginal statistics are matched for $p > q$. It follows that the reconfigured channel achieves the capacity corresponding to $\mathbf{M}(D, p)$ for $p \le q$, but the capacity may deviate a little for $p > q$ especially at high SNR's since the reconfigured channel always has a kronecker (separable) structure whereas $\mathbf{M}(D, p)$ is non-separable for $p > q$ [4]. With this qualification, we have the following.

Corollary 3: In randomly sparse physical channels, the (capacity maximizing) Ideal MIMO Channel at any transmit SNR can be created by choosing $d_{r,opt}$ and $d_{t,opt}$ in (11) corresponding to p_{opt} defined in (10).

Remark 3: **Three Canonical Array Configurations**. Three channel configurations are highlighted in Fig. 1 corresponding to $N = D = 25$: BF: $\mathbf{H}_{v,bf} \leftrightarrow p_{bf} = p_{min} = 1$; IDEAL: $\mathbf{H}_{v,id} \leftrightarrow p_{id} = \sqrt{D} = \sqrt{N}$; and MUX: $\mathbf{H}_{v,mux} \leftrightarrow p_{mux} = p_{max} = N$. The BF and MUX configurations represent the Ideal MIMO Channel for $\rho < \rho_{low}$ and $\rho > \rho_{high}$, respectively. As evident from the figure, the IDEAL configuration is a good approximation to the Ideal MIMO Channel for $\rho \in (\rho_{low}, \rho_{high})$ (the Ideal MIMO capacity does not vary much in this range). Thus, from a practical viewpoint, these three configurations suffice for adapting array configurations to maximize capacity over the entire SNR range.

A. Numerical Example

We present a numerical example to illustrate the creation of the three canonical channel configurations, $\mathbf{H}_{v,mux}$, $\mathbf{H}_{v,id}$, and $\mathbf{H}_{v,bf}$, by adapting the antenna spacings as in Thm. 2. We consider $N = D = 25$ ($\gamma = 1$) and first generate the AoA's and AoD's $(\theta_{r,\ell}, \theta_{t,\ell}) \in [-1/2, 1/2]^2$ for $L = 25$ paths, where the AoA/AoD's of different paths are randomly distributed over the entire angular spread. This defines $\mathbf{H}_{mux}$

environment for $d_{t,mux} = d_{r,mux} = d_{max} = \lambda/2$, without loss of generality (Fig. 1(c)). These AoA/AoD's are then fixed and the capacities of the different channel configurations are estimated via 200 realizations of the scattering environment simulated using (2) by independently generating $\mathcal{CN}(0,1)$-distributed complex path gains. The random locations of the D paths are illustrated in Fig. 3(a), which shows the contour plot of $\mathbf{\Psi}_{mux}$. Using (11) and Rem. 3, the spacings for $\mathbf{H}_{v,bf}$ are $d_{t,bf} = d_{t,mux}/N$ (Fig. 1(e)) and $d_{r,bf} = d_{r,mux}$ (Fig. 1(c)), whereas the spacings for $\mathbf{H}_{id}$ are $d_{t,id} = d_{r,id} = d_{r,mux}/\sqrt{N}$ (Fig. 1(d)). The contour plots of the resulting $\mathbf{\Psi}_{id}$ and $\mathbf{\Psi}_{bf}$ are illustrated in Figs. 3(b) and (c) and confirm the sizes of the non-vanishing sub-matrices $\tilde{\mathbf{H}}_v$ in Thm. 2 (the corresponding $\tilde{\mathbf{\Psi}}_{bf}$ and $\tilde{\mathbf{\Psi}}_{id}$ in Fig. 3 are approx. $N \times 1$ and $\sqrt{N} \times \sqrt{N}$; compare also with Fig. 2). The numerically estimated capacities for the three configurations, corresponding to the theoretically optimal uniform-power inputs in Cor. 1, are plotted in Fig. 3(d) along with the theoretical curves (Fig. 1(b)) using (9). We note that the uniform-power inputs are not optimal for the simulated channel since its not regular (the paths locations remain fixed) and we expect the agreement to be even more striking if averaging is done over locations of paths as well.

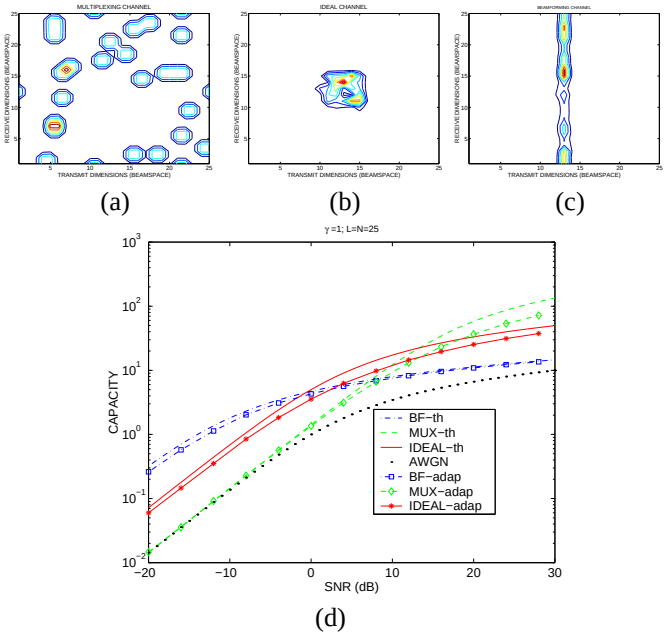

Fig. 3. (a)-(c): Contour plots of $\mathbf{\Psi}$ for the three canonical configurations in a physical environment with with N=D=25 randomly distributed paths; (a) $\mathbf{\Psi}_{mux}$; (b) $\mathbf{\Psi}_{id}$; (c) $\mathbf{\Psi}_{bf}$. (d) The numerical capacities of the three configurations with uniform power inputs, along with the theoretical values.

B. Discussion

Thm. 2 establishes the equivalence of MIMO channels created with reconfigurable antenna arrays with the Ideal MIMO Channel in Thm. 1 by averaging over all randomly sparse channels with D scattering paths. While the channels in Thm. 2 and Thm. 1 are *regular* [4] over the non-vanishing transmit dimensions, in practice, we will encounter a particular sparse scattering environment, as illustrated in the numerical example in Fig. 3, which will result in *irregular* channels in general (the non-vanishing transmit eigenvalues will be non-uniform). In such cases, optimizing the input power allocation, as in (5), will be beneficial and the capacity gains due to array configurations would be smaller. To quantify the gains due to adaptive array configurations at low SNR's, we compare $\mathbf{H}_{mux}$ with $\mathbf{H}_{bf}$. $\mathbf{H}_{mux}$ represents the optimal array configuration at high SNR's and its capacity as a function of ρ reflects the performance if we optimized the input, as in (5), while keeping the antenna spacings fixed. $\mathbf{H}_{bf}$ on the other hand reflects capacity optimization at low SNR's by adapting spacings. The following result quantifies the capacity gains due to reconfigurable arrays which we state without proof.

Proposition 2: Let C_{mux} and C_{bf} denote the capacities of $\mathbf{H}_{mux}$ and $\mathbf{H}_{bf}$. The capacity gain in the low-SNR regime due to reconfigurable arrays is given by

$$CG = \lim_{\rho \to 0} \frac{C_{bf}(N, D, \rho)}{C_{mux}(N, D, \rho)} = \frac{D}{\lambda_{t,max}} \leq N \qquad (12)$$

where $\lambda_{t,max}$ denotes the largest transmit eigenvalue of $\mathbf{H}_{mux}$ and the largest gain N is achieved for regular channels.

Remark 4 (Physical Source-Channel Matching): The capacity maximizing input for fixed spacings (see (5)) allocates all power to the strongest virtual direction at low ρ. With reconfigurable arrays, d_t is decreased with ρ to concentrate channel power in fewer non-vanishing virtual transmit beams: the number of non-vanishing transmit eigenvalues gets smaller but their size gets bigger. This reflects a form of source-channel matching: the rank of the optimal input is better-matched to the rank of $\mathbf{H}_v$. As a result, compared to optimal power allocation with fixed spacings, no channel power is wasted as the multiplexing gain is optimally reduced through $d_t \leftrightarrow p$. Physically, as d_t is decreased fewer data streams (p) are transmitted over a corresponding number of spatial beams, whereas the width of the beams gets wider (see Figs. 1(c)-(e)). In effect, for any p, N/p closely spaced antennas coherently contribute to each beam to sustain a constant power over the N/p-times wider beamwidth.

REFERENCES

[1] Í. E. Telatar, "Capacity of Multi-antenna Gaussian Channels," *AT& T-Bell Labs Internal Tech. Memo.*, June 1995.

[2] G. J. Foschini, M. J. Gans "On Limits of Wireless Communications in a Fading Environment when using Multiple Antennas," *Wireless Per. Comm.*, vol. 6, no. 3, pp. 311-335, 1998.

[3] A. Sayeed, V. Raghavan, J. Kotecha, "Capacity of Space-Time Wireless Channels: A Physical Perspective," *IEEE Inform. Th. Workshop*, 2004.

[4] A. Tulino, A. Lozano, and S. Verdu, "Impact of Antenna Correlation on the Capacity of Multiantenna Channels," *IEEE Trans. Inform. Th.*, July 2005.

[5] A. M. Sayeed, "Deconstructing Multi-antenna fading channels," *IEEE Trans. Signal Processing*, vol. 50, no. 10, pp. 2563-2579, Oct. 2002.

[6] V. V. Veeravalli, Y. Liang, A. M. Sayeed, "Correlated MIMO Wireless Channels: Capacity, Optimal Signaling, and Asymptotics," *IEEE Trans. Inform. Th.*, June 2005.

[7] Y. Zhou, M. Herdin, A. Sayeed, E. Bonek, "Experimental Study of MIMO Channel Statistics and Capacty Via the Virtual Channel Representation, *submitted to the IEEE Trans. Wireless Commun.*

[8] T. Muharemovic, A. Sabharwal, B. Aazhang, "Antenna Packing in Low Power Systems: Communication Limits and Array Design," *Submitted to IEEE Trans. Inform. Th.*, Jan. 2005.

[9] G. Barriac, U. Madhow, "Space-time communication for OFDM with implicit channel feedback," *IEEE Trans. Inform. Theory,*, Dec. 2004.